EUROPEAN CONTRIBUTIONS TO THE BEAM SOURCE DESIGN AND R&D OF THE ITER NEUTRAL BEAM INJECTORS

P. MASSMANN(1), P. BAYETTI(1), J. BUCALOSSI(1), C. DESGRANGES(1), E. DI PIETRO(3), P. FRANK(2), M. FUMELLI(1), Y. FUJIWARA(4), M. HANADA(4), B. HEINEMANN(2), R. S. HEMSWORTH(1), T. INOUE(3), C. JACQUOT(1), W. KRAUS(2), Y. OKUMURA(4), F. PROBST(2), A. SIMONIN(1), E. SPETH(2), R. TRAINHAM(1) and O. VOLLMER(2)

(1) Association EURATOM - CEA Cadarache, DRFC / SCCP, 13108 ST PAUL LEZ DURANCE Cedex, France

(2) Association EURATOM - Max Planck Institut für Plasmaphysik, 85748 GARCHING, Germany

(3) ITER JCT, Naka JWS, 801-1 Mukouyama, Naka-machi, Naka-gun, Ibaraki-ken, Japan 331-0193

(4) Japan Atomic Energy Research Institute JAERI, 801-1 Mukouyama, Naka-machi, Naka-gun, Ibaraki-ken, Japan 331-0193

Abstract

The paper reports on the progress made by the European Home Team in strong interaction with the ITER JCT and JAERI regarding several key aspects of the beam source for the ITER injectors:

- integration of the SINGAP accelerator into the ITER injector design. This is a substantially simpler concept than the MAMuG accelerator of the ITER NBI 'reference design', which has potential for significant cost savings, and which avoids some of the weaknesses of the reference design such as the need for intermediate high voltage potentials from the HV power supply and pressurised gas insulation.
- high energy negative ion acceleration using a SINGAP accelerator
- long pulse (i.e. >1000 s) negative ion source operration in deuterium
- RF source development, which could reduce the scheduled maintenance of the ITER injectors (as it uses no filaments), and simplify the transmission line and the auxiliary power supplies for the ion source

1. INTRODUCTION

The overall design of the ITER Neutral Beam Injection (NBI) system [1] has advanced to a level which gives confidence that such a system can be feasible. Naturally, there have been and will be adaptations to the design and the R&D will and should continue, until the design is frozen for construction, in order to demonstrate / improve reliability and to reduce the system costs. The adaptation of the reference design [1] using a gas insulated beam source (GIBS) to High Voltage (HV) insulation by vacuum has been provoked by recent measurements indicating the ionising effect of the neutron and gamma radiation on the insulating, pressurised gas which is likely to cause power losses between 0.1 - 1 MW [2]. Like the GIBS design, the reference design of the vaccum insulated beam source (VIBS) [3] uses Multi-Aperture Multi-Grid (MAMuG) acceleration to 1 MV in 5 steps of 200 kV. The SINGAP (SINgle GAP - SINGle APerture) beam source (SIBS) [4] is well suited to vacuum insulation, hence this concept may be seen as a compatible alternative to the VIBS design with promising potential for simplification and possible cost reduction.

In the first part of this paper we report on the progress made in the integration of the SIBS concept into the ITER NBI system. Subsequently some of the relevant R&D issues are addressed. We report on the latest activities regarding the 1 MV SINGAP acceleration and the demonstration of reliable and stable long pulse D^- source operation, the latter being a collaborative effort between JAERI and CEA. The development of an RF driven negative ion source undertaken in a collaboration between IPP Garching and CEA is aimed at the longer term as it offers the possibility of reduced maintenance and increased simplicity of the ion source, its power supplies and the HV transmission line. The progress regarding this development will be reviewed in the last part of this paper.

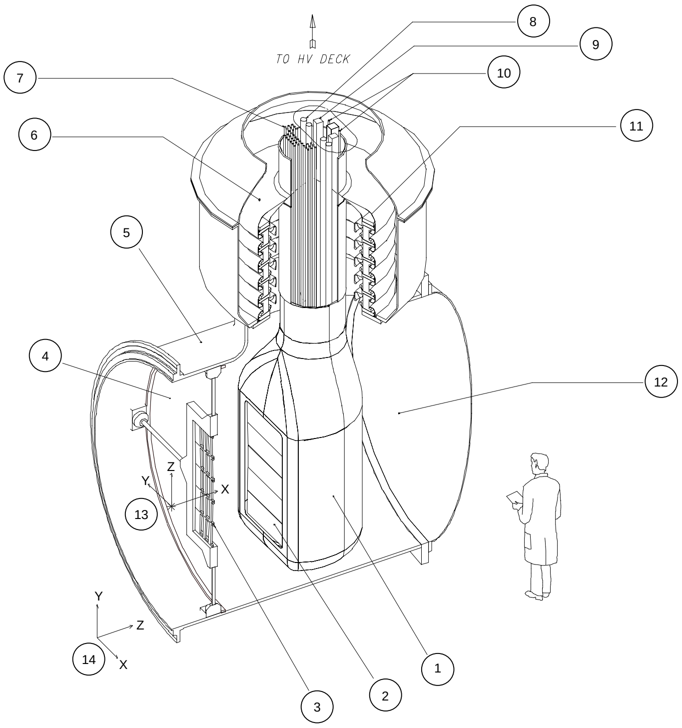

FIG. 1
Isometric View of the SINGAP Beam Source (SIBS)

(1) HV Source (-1 MV)
(2) Pre-Acceleration Grid
(3) Movable SINGAP Electrode
(4) High Transparency Screen
(5) Vacuum Vessel
(6) Insulating Pressurised Gas
(7) Filament Busbars
(8) Coolant Lines
(9) High Current Bus Bars
(10) Gas Lines
(11) HV Bushing
(12) Vacuum
(13) ITER Coordinates
(14) SIMION Coordinates

2. BEAM SOURCE DESIGN

2.1. Concept

The acceleration to 1 MV in one single gap is expected to yield a considerable simplification and cost reduction of the HV components, i.e. the transmission line, the bushing and the power supplies since the HV power supply does not need to provide intermediate potentials. To benefit fully from this accelerator concept it is proposed to suspend the source and pre-accelerator assembly from the high voltage bushing and attach the post-acceleration SINGAP electrode independently inside the beamline vessel. It is also expected that adequate steering of the SINGAP 'hyper beamlets' may be obtained by offsetting the SINGAP apertures [4] rather than with electrostatic beam steering plates as foreseen in the reference design. The design allows also for controlled displacement of the SINGAP electrode, which results in a horizontal steering of the whole beam, and which can be used to compensate for errors in horizontal alignment.

2.2. The SINGAP Beam Source (SIBS)

2.2.1. HV Bushing

An isometric view of the SINGAP beam source is shown in Fig. 1 and an assembly of the five stage SINGAP bushing in Fig. 2. The auxiliary supplies for the ion source, extractor (10 kV) and pre-accelerator (100 kV) are to be provided by power supplies on the HV deck and the leads fed through the centre conductor of the HV transmission line together with the other service lines (water and gas).

To minimise the risk of HV breakdowns the guidelines of Table 1, which have been established in detail in [5], have been adopted. Special attention has been paid to the electric field at the cathode triple points of the insulator rings where the shape of the electrostatic screen ensures field strengths < 1 kV/cm. To avoid secondary electron generation the bombardment of the insulator by primary electrons is prevented by an overlap of the cathode and anode side of the screens. At the pressurised gas side acceptably low field concentrations are achieved by the median screens which are made up of two halves and which can be clipped onto clamps holding together and centring the ceramic rings with respect to the intermediate metal flanges.

TABLE I. GUIDLINES FOR BUSHING AND ELECTROSTATIC SCREEN DESIGN

Issue	Target Value	Remedy
insulator electron bombardment	negligible	metal screen overlap
stress at negative triple points	< 1 kV/cm	metal screen shape
stress at cathode areas, vacuum	≤ 50 kV/cm (bushing)	maximise curvature radius
	≤ 30 kV/cm (ion source)	
insulator surface stress, vacuum	< 15 kV/cm	optimise curvature and distance
pressure * distance, vacuum	$p*d < 3\ 10^{-3}$ Pa	optimise pumping
stress at cathode areas, gas side	< 60 - 100 kV/cm	optimise curvature, gas type, pressure

In order to combine low degassing, low secondary electron emission, radiation resistance and small differential thermal expansion a combination of IEC C221 porcelain and titanium is proposed. As seals between the insulator stages spring energised metal O-rings may be used directly between ceramic and metal as envisaged by the Japanese Home Team.

It is important to note that the metal sealed ceramic structure forms a part of the primary tritium boundary, and this must be qualified for this purpose. The insulating gas, which also acts as the secondary confinement boundary for the T_2, and a guard gas, must exhibit adequate radiation properties and, in case of a leak, must be acceptable to the tritium handling system. Dry N_2 appears to be a good candidate [6].

A preliminary optimisation of the bushing design has been carried out with the SIMION 6 electrostatic field and particle code [7]. Although this code does not treat dielectrics (and space charge) it has proven a very useful tool as it allows rapid changes of geometry. The resulting design was then studied with the 3D 'Opera' code from Vector Fields [8]. Due to dielectric refraction the 'Opera' code calculates slightly higher fields near the triple points, but which are still within the design guidlines. The screening of the cathode triple point induces field concentrations on the ceramic surface which are higher than generally found in accelerators of present day injectors. This may be reduced by some fine tuning of the screen and insulator shape or by a slight increase of the insulator height.

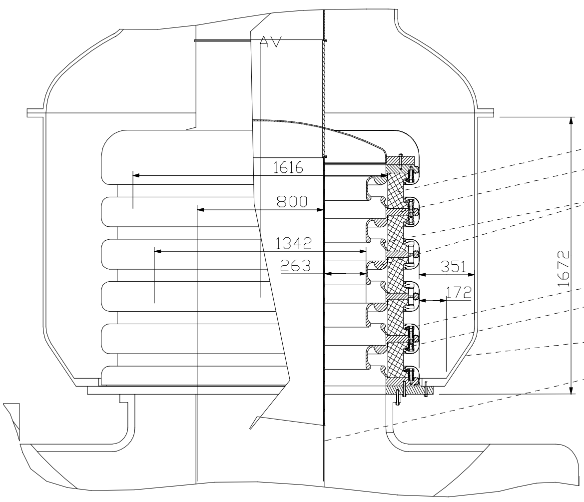

FIG. 2
The SINGAP Bushing
(1) IEC C221 Porcelain, (2) Titanium Flange
(3) Electrostatic Screen, (4) Median Screen
(5) Clamp, (6) Gas Compartment (N_2)
(7) Centre Conductor (-1 MV)

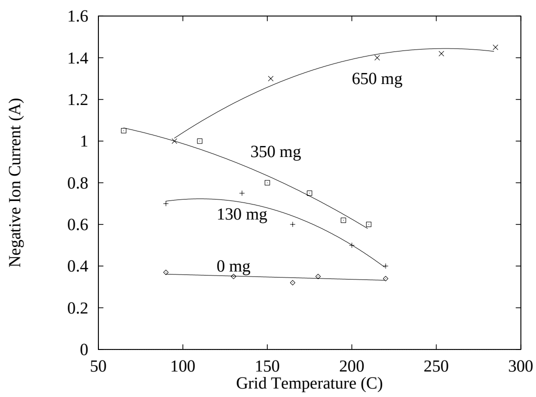

FIG. 3
Effects of Plasma Grid Temperature and Caesium Quantity
Note that the temperature varies together with time

2.2.2. Electrostatic Field Distribution in the Beam Source Vessel

The SIBS concept requires only one electrostatic screen around the ion source to reduce field stresses. The SINGAP fields are typically weak and long ranged. Therefore, the source screen has to be shaped in such a way that the beam trajectories in the post-acceleration gap are not adversely effected. Consistent with the configuration for the 'proof of principle' calculations [4] the screen side facing the SINGAP electrode forms an extension of the plane defined by the pre-accelerator grid support flange. Downstream the 0 V potential plane of the SINGAP electrode is extended towards the tank walls. To retain optimum pumping a screen structure made of high transparency wire mesh is proposed.

The electrostatic field in the source vessel (100 m^3) has been modelled with the 3D SIMION 6 code. The analysis shows a constant field of 27 kV/cm across the whole of the post-acceleration area. Furthermore, the highest field stresses found are only 27 kV/cm, below the guidlines.

2.2.3. Stripped Electron Deposition

To assess the nature of the electron losses an analysis has been carried out with the Vector Fields code of the transport of stripped electrons in the SINGAP accelerator [9]. The geometric input data are taken from [10] (Table II), the distribution of stripping losses along the accelerator (40 A beam, source pressure 0.3 Pa) from [11].

TABLE II. GEOMETRIC GRID PARAMETERS

Item	Aperture Diameter [mm]	Thickness [mm]	Gap Length [mm]
plasma grid	14	6	-
extractor	10	10	5
pre-accelerator	14	20	35
post-accelerator	115 (hor) x 324 (vert)	20	350

The loss distribution along the electrode stack resulting from stripped electrons has been determined for two cases: (1) no electron suppression in the pre-accelerator, in which case 80% of the electrons stripped in the pre-acceleration gap enter the post-accelerator and (2) with electron suppression (permanent magnets in the pre-accelerator), in which case none of the electrons stripped in the pre-accelerator enter the post-accelerator. The results are listed in Table III.

TABLE III. STRIPPING LOSS POWER DISTRIBUTION ALONG THE ACCELERATOR

Component	Losses - Assumption (1)		Losses - Assumption (2)	
	Power Fraction [%]	Power Loading [MW]	Power Fraction [%]	Power Loading [MW]
extraction grid	0.03	0.012	0.03	0.012
pre-acceleration grid	0.06	0.025	0.32	0.129
past pre-acceleration grid	8.58	3.42	2.7	1.08
TOTAL	8.65	3.46	3.05	1.2
	Losses - Assumption (2a)		Losses - Assumption (2b)	
SINGAP electrode	12	0.13	<1	0.01
neutraliser (and / or RID)	73	0.79	98 – 99	1.06
tank	15	0.16	<1	0.01

Retaining assumption (2), the trajectories of a sample of electrons launched at various positions along the post-acceleration gap have then been calculated yielding the electron loss deposition downstream of the pre-accelerator for two cases of magnetic plasma grid filter field (Table III):

(2a) reference design with a current of 6 kA through the plasma grid giving a spatial field extension along the beam of ~ 38 to 7 G which causes a stripped electron deflection of up to 20° and (2b) the magnetic filter is produced locally (e.g. by permanent magnets in the plasma grid), in which case the only magnetic field in the accelerator is the stray field from the tokamak (~ 4 G along and ~1 G transverse to the beam).

The results of the analysis indicate that by applying an efficient electron suppression in the pre-accelerator the loss power due to stripped electrons may be reduced by nearly a factor 3. The effect of a localised plasma grid filter created by permanent magnets instead of a large current through the grid would be beneficial for the electron deposition as nearly all the electron losses will be dumped safely on components (neutraliser and / or RID) which are designed to handle these powers. Moreover, the experiments at Cadarache suggest that the long extension of the filter field also deflects the ions [4, 12]. It is therefore proposed to re-design the plasma grid filter using water cooled permanent magnets immersed on, or inside, the plasma electrode.

3. BEAM SOURCE R&D

3.1. Activities on the Cadarache 1 MV Experiment

3.1.1 Beam Acceleration

Results regarding beam acceleration have been reported recently [12]. The highest beam energy obtained is 860 keV (45 mA H^-) and the highest current 106 mA D^- (630 keV). The amount of co-accelerated electrons is negligible and the overall beam divergences range between 8 and 12 mrad. Raising the energy has been hampered by the failure of two (out of nine) insulator rings in the 1 MV bushing. The faulty rings made of fibre glass reinforced epoxy have now been replaced using quartz powder charged epoxy moulded in vacuum. Both have been tested succesfully for HV holding up to 150 kV leaving a good safety margin above the nominally required 111 kV.

In parallel, an insulator ring (442 mm ID, 718 mm OD, 94 mm height) made of extruded, commercial IEC C120 porcelain with epoxy glued titanium inserts has been fabricated, using a design largely identical to that of the epoxy rings. The porcelain module has been HV tested successfully up to 200 kV. It is found that HV breakdowns in vacuum are scarce. The actual conditioning work consists, at each voltage, of reducing the continuous dark current between the metal electrostatic screens, typically 5 to 10 mA initially, to < 1 mA before increasing the applied voltage, and so on. Practically dark current free HV holding at 130 kV was achieved after about 130 5 s pulses.

3.1.2 Source Development

For future applications and to comply with the ITER injector specifications a new prototype negative ion source module (22 cm^H x 13 cm^W x 18 cm^D) has been built. Permanent magnets are used in a novel design to provide both confinement and magnetic filter in this 'Drift Source', which is designed to allow horizontal or vertical stacking to produce larger size sources. First results are very promising yielding pre-accelerated 50 kV beams of 20 mA/cm^2 D^- at source pressures of 0.15 Pa. The details of this development have been presented in [13].

3.2. Long Pulse Source Experiments

In a JAERI / CEA collaboration a small scale ‘Kamaboko III’ ITER concept source is being tested in long pulse operation on the Cadarache MANTIS (Multi-Ampere NegaTive Ion Source) test bed. Results regarding this activity are presented elsewhere at this conference [14].

To comply with the ITER specifications this source has to deliver ≥ 20 mA/cm^2 D^- at ≤ 0.3 Pa with a ratio of co-extracted electrons < 1. The stability of the extracted ion beam must be assured for ≥1000 s. Reaching the specifications requires Cs admixture of the plasma discharge and a plasma electrode temperature of 200 - 300 ^{0}C. Fig. 3 shows the relation between plasma grid temperature, source on time, caesium quantity and negative ion yield. This is an important confirmation of results found earlier [15]. Apparently, a minimum quantity of Cs is required in this type of source to reach optimum and stable performance. Once this has been established it can be maintained for long pulses, but after a conditioning period of several days.

Two different designs of plasma grids have been produced by the Japanese Home Team which allow continuous operation at the required temperatures with conventional (low pressure) water cooling. The two designs differ in the way the thermal barriers are introduced between the exposed grid body and the water channels. The 'frame cooled' design uses a corrugated thermal bridge connecting the edge of the CuCrZr grid to a water cooled frame. In the 'actively cooled' design the Mo grid is traversed by Cu water channels and the thermal barriers are established by stainless steel inlays between the grid and the cooling channels.

It has been found that both grids are able to sustain stable temperatures of 200 - 300 ^{0}C. With the 'frame cooled' grid 1000 s arc pulses at 0.2 Pa with intermittent 10 s D^- ion beam (< 30 kV) pulses have been demonstrated successfully. Full 1000 s D^- pulses will be attempted in silent hours (to limit radiation exposure) once the remote control system [16] is fully implemented.

3.3. RF Negative Ion Source

The aim of the IPP Garching / CEA collaboration is to develop an RF driven negative ion source which meets the ITER beam source specifications (see above) and simultaneously fulfils the demand for low maintenance due to the absence of filaments. The experimental work is being carried out with support from Cadarache on the Garching BATMAN (BAvarian Test MAchine for Negative Ions) test stand. Recent results regarding this development have been reported in [17, 18, 19].

To gather results quickly the experiments started with a readily available ASDEX Upgrade type II source [20] which was modified for negative ions by adding a Cs feed and a magnetic filter in front of the plasma grid [17]. Because of its external antenna this source has no provisions for magnetic confinement on the side walls and permanent magnets are only on the back plate. The highest negative ion yields are about 8.5 mA/cm^2 H^- at elevated pressures around 2.4 Pa with an admixture of both Cs and Ar. The dependence of the yield on gas pressure for various conditions is shown in Fig. 4. The enhancement in yield (up to a factor 8 compared to no admixture) with the two additives is strongest at low filling pressures. It is suspected that the enhancement with Cs is due to a decrease of the work function on the plasma electrode whereas the additional boost with argon is caused by a measured increase of the electron density and a likely change in the electron energy

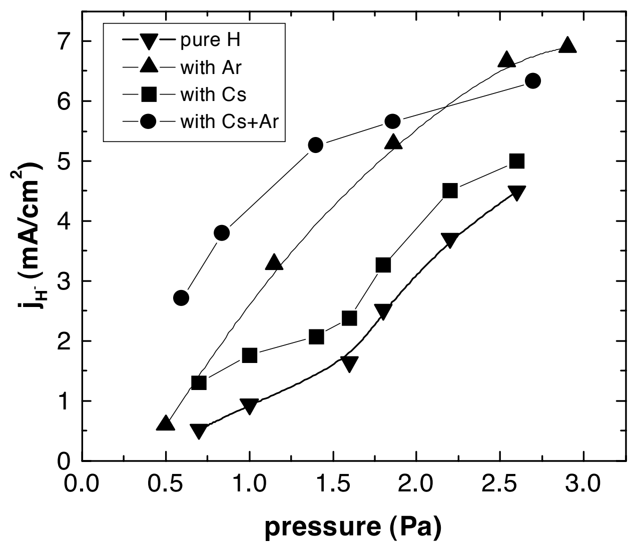

Fig. 4 IPP RF Source Type II - Extracted H^- Current Density vs Source Pressure (P_{RF} = 100 kW)

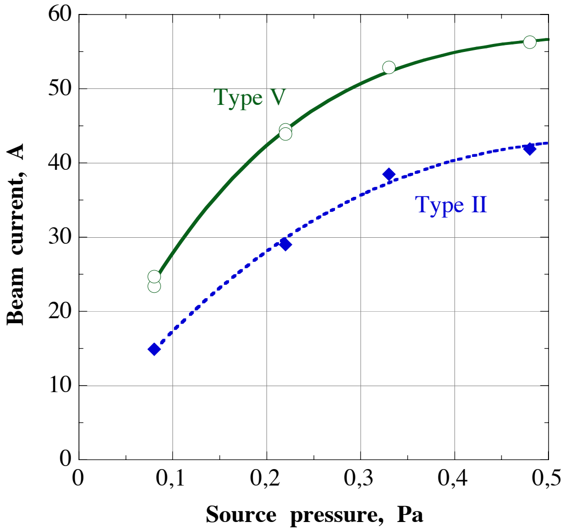

Fig. 5 IPP RF Sources Types II and V - Extracted Positive Ion Current vs Pressure (P_{RF} = 60 kW)

Fig. 6

Negative Ion RF Source (IPP - CEA Collaboration) - Cut-away of Large Area / High Transparency Extraction Grid

In spite of the additional electron traps and suppression magnets the original 37% transparency of the JET PINI grids which formed the elements for this negative ion extraction and acceleration system could be maintained

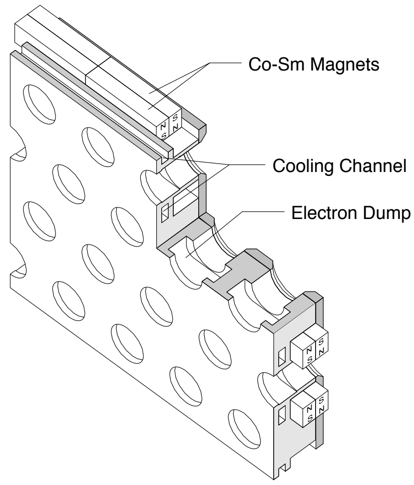

distribution. Despite of this enhancement the highest yields at the lowest pressures around 0.5 Pa are still an order of magnitude below the ITER NBI requirements which are ~ 30 mA/cm^2 at ≤ 0.3 Pa in hydrogen.

Not unexpectedly the plasma confinement has to be improved and, probably, the electron temperature in the source reduced. Therefore an RF type V source with permanent magnets around the metal side walls and an internal 3 turn antenna has been prepared and, for the moment, run in positive ion mode to compare with the standard type II source [20]. The positive ion beam currents from the two types are compared in Fig. 5. It can be seen that the plasma confinement has indeed improved as the same ion current can be extracted at half the pressure (< 0.2 Pa) for the same input power. Experiments should now continue with adding a suitable magnetic filter field to favour negative ion production.

The experiments with the RF type II negative ion source have been done with a medium size plasma grid (69 cm^2, 45 apertures) to allow direct comparison with the filamented source used at Cadarache. However, to progress towards higher currents and to qualify the negative ion distribution of the RF source a large area negative ion extraction and acceleration system has been designed and is presently under manufacture [19]. This was achieved by modifying an existing PINI extraction system (390 cm^2, 774 apertures), adding a magnetic filter in front of the plasma grid and replacing the deceleration grid by a new negative ion extraction grid. A drawing of this is shown in Fig. 6.

4. SUMMARY AND CONCLUSIONS

4.1. Design

Progress has been made integrating the SINGAP concept into the ITER injector design. Although some ‘fine tuning’ is still necessary the design of the 1 MV SINGAP bushing, possibly the most challenging component of the accelerator, gives confidence that the HV holding and mechanical requirements can be met. A detailed design should now follow.

With the proposed screens around the ion source and at the SINGAP electrode the global electric field distribution in the beam source vessel seems satisfactory. The 3D modelling shows 'comfortable' stress concentrations below 30 kV/cm. In the post-acceleration area the global field is constant so that the SINGAP optics will be determined (as intended) by the pre- and post- accelerator.

A horizontally adjustable SINGAP electrode has been proposed for alignment correction. This seems necessary from experience with present day injectors, and a design using no bellows is proposed.

The calculations of the particle trajectories in the accelerator show that electrons stripped in the pre-accelerator should be suppressed locally.

The application of a local plasma grid filter produced by water cooled permanent magnets will be beneficial for all designs as it reduces the undue deflection of electrons and ions in the accelerator.

4.2. R&D

The Cadarache porcelain insulator has demonstrated breakdown free voltage holding up to 200 kV, far above the nominal voltage. It is thus possible to hold off 200 kV in vacuum across a distance of only 94 mm, less than half that used in the ITER bushing design.

The prototype ‘drift source’ module has successfully demonstrated its potentials which should now allow acceleration of a D^- ion beam of ITER relevant current densities up to 1 MV.

On the MANTIS test stand 1000 s deuterium source pulses have been demonstrated. Both JAERI long pulse grid designs can operate at optimum negative ion production conditions. Beam extraction in deuterium at ITER relevant parameters has been limited to intermittent operation because of induced neutron radiation, but long deuterium beam pulses are expected shortly using a remote control system operated via the Internet.

Overall, steady progress has been made in the development of the RF negative ion source. Almost all the ‘ingredients’ for running a large area RF negative ion source have now been gathered which could allow substantial progress in the near future.

REFERENCES

[1] HEMSWORTH, R.S. et al, ITER Neutral Beam Injector Design, 16th IAEA Fusion Energy Conference, Montreal, 7 - 11 October 1996, Vol II p. 927

[2] HODGSON, E.R. and MOROÑO, A., Radiation Induced Power Loss in Insulating Gases for ITER NBI Systems, 20th SOFT, Marseille, 7 - 11 September 1998, Vol I p. 295

[3] DI PIETRO, E. et al, The Vacuum Insulated Beam Source for the ITER Neutral Beam Injection System, 20th SOFT, Marseille, 7 - 11 September 1998, Vol I p. 407

[4] MASSMANN, P. et al, SINGAP Acceleration of High Energy Negative Ion Beams, 16th IAEA Fusion Energy Conference, Montreal, 7 - 11 October 1996, Vol III p. 571

[5] BAYETTI, P., VHTP in Support of the Design of the Neutral Beam System, Final Report Contract ERB 5004 CT 97 0113 (NET/97-461) - Part of the ITER Neutral Beam Injector Design (Design Task N53 TD 17 FE - D322), September 1998

[6] HODGSON, E.R. and MOROÑO, A., Radiation Induced Leakage Currents for Voltages up to 50 kV for 0.5 m Electrode Separation, 2nd Joint JA - EU Workshop on Neutral Beam Injectors - 'Super JDC', Dublin City University, 23 - 24 March 1998

[7] DAHL, D.A., SIMION 3D Version 6, 43 ed. ASMS Conf. on Mass Spectrometry and Allied Topics, Atlanta, p. 717

[8] SIMKIN, J., Vector Fields Ltd., 24 Bankside, Kidlington OX5-1JE, U.K.

[9] BUCALOSSI, J., "Where do the stripped electrons go?" in Final Report Contract ERB 5004 CT 97 0113 (NET/97-461) - Part of the ITER Neutral Beam Injector Design (Design Task N53 TD 17 FE - D322), September 1998

[10] SIMONIN, A. et al, Extraction System Development and Stray Electron Study for High Intensity Negative Ion Based NBI, 19th SOFT, Lisbon, 16 – 20 September 1997

[11] HANADA, M., JAERI, private communication

[12] DESGRANGES, C. et al, Beam Optics of the SINGAP 1 MeV 100 mA D^- DC Accelerator, 20th SOFT, Marseille, 7 - 11 September 1998, Vol I p. 347

[13] SIMONIN, A. et al, The Drift Source: A Negative Ion source Module for Multi-Ampere Ion Beams, 20th SOFT, Marseille, 7 - 11 September 1998, Vol I p. 363

[14] JACQUOT, C. et al, this conference, poster FTP/19

[15] MIYAMOTO, N. et al, Negative Ion Source Development at JAERI, 2nd Joint JA - EU Workshop on Neutral Beam Injectors - 'Super JDC', Dublin City University, 23 - 24 March 1998

[16] TRAINHAM, R. and JACQUOT, C., Long Pulse Extraction of Negative Ion Beams from the KAMABOKO Ion Source, 20th SOFT, Marseille, 7 - 11 September 1998, Vol I p. 367

[17] FRANK, P. et al, Progress of the BATMAN RF Source for Negative Hydrogen Ions, 20th SOFT, Marseille, 7 - 11 September 1998, Vol I p. 429

[18] KRAUS, W. et al, An RF Source Optimized for Low Pressure Operation, 20th SOFT, Marseille, 7 - 11 September 1998, Vol I p. 441

[19] HEINEMANN, B. et al, Large-Area, High-Transparency Extraction System for Negative Ions, 20th SOFT, Marseille, 7 - 11 September 1998, Vol I p. 433

[20] VOLLMER, O. et al, Commissioning and Performance of the New ASDEX Upgrade Neutral Beam Injector, 20th SOFT, Marseille, 7 - 11 September 1998, Vol I p. 449